Inhibition of endothelial Nox2 activation by LMH001 protects mice from angiotensin II-induced vascular oxidative stress, hypertension and aortic aneurysm

Article

Published Version

Inhibition of endothelial Nox2 activation by LMH001 protects mice from angiotensin II-induced vascular oxidative stress, hypertension and aortic aneurysm

Lampson M. Fan [a], Fangfei Liu [b], Junjie Du [c,d], Li Geng [b,d], Jian-Mei Li [b,d,*]

[a] Department of Cardiology, Royal Wolverhampton NHS Trust, UK
[b] School of Biological Sciences, University of Reading, UK
[c] Department of Cardiovascular Surgery, Nanjing Medical University, PR China
[d] Faculty of Health and Medical Sciences, University of Surrey, UK

ARTICLE INFO

ABSTRACT

Endothelial oxidative stress and inflammation attributable to the activation of a Nox2-NADPH oxidase are key features of many cardiovascular diseases. Here, we report a novel small chemical compound (LMH001, MW = 290.079), by blocking phosphorylated p47^{phox} interaction with p22^{phox}, inhibited effectively angiotensin II (AngII)-induced endothelial Nox2 activation and superoxide production at a small dose (IC50 = 0.25 μM) without effect on peripheral leucocyte oxidative response to pathogens. The therapeutic potential of LMH001 was tested using a mouse model (C57BL/6J, 7-month-old) of AngII infusion (0.8 mg/kg/d, 14 days)-induced vascular oxidative stress, hypertension and aortic aneurysm. Age-matched littermates of p47^{phox} knockout mice were used as controls of Nox2 inhibition. LMH001 (2.5 mg/kg/d, ip. once) showed no effect on control mice, but inhibited completely AngII infusion-induced excess ROS production in vital organs, hypertension, aortic walls inflammation and reduced incidences of aortic aneurysm. LMH001 effects on reducing vascular oxidative stress was due to its inhibition of Nox2 activation and was abrogated by knockout of p47^{phox}. LMH001 has the potential to be developed as a novel drug candidate to treat oxidative stress-related cardiovascular diseases.

Endothelial oxidative stress and inflammation attributable to the excess production of reactive oxygen species (ROS) by a Nox2-containing nicotinamide adenine dinucleotide phosphate oxidase (NADPH oxidase, or Nox) is involved in many cardiovascular diseases such as hypertension, atherosclerosis, aortic aneurysms and heart failure [1–3]. The NADPH oxidase is a complex enzyme of several regulatory subunits, e.g., p40^{phox}, p47^{phox}, p67^{phox} and rac1 and a cytochrome b558 (containing a catalytic Nox subunit and a p22^{phox} subunit) [1,4]. So far, seven isoforms of Nox (Nox1-5 and Duox 1–2) have been reported. Among them, Nox2 is highly expressed in vascular endothelial cells and phagocytes [3,5]. Endothelial Nox2 has a low basal activity under the physiological conditions. However, when endothelial cells face challenge, such as AngII, inflammatory cytokines and high glucose, endothelial Nox2 is activated. Excessive $O_2^{\cdot-}$ production by Nox2 results in endothelial dysfunction and oxidative damage.

The p47^{phox} is a primary regulator of Nox2 enzyme [4,6]. In the vascular system, p47^{phox} phosphorylation and binding to p22^{phox} are essential for AngII-induced endothelial Nox2 activation and ROS production [7]. In animal models, selective knockout of p47^{phox} or Nox2 can prevent the development of oxidative stress-related vascular diseases which makes Nox2 an attractive target for pharmacological intervention [8,9]. During the past decades, several chemical compounds of Nox2 inhibitors have been reported [10–14]. However, there are concerns in their clinical application because leucocyte Nox2 activation is crucial for host defence. It is essential therefore, that any potential anti-Nox2 therapy when used at an effective dose to treat vascular oxidative stress would not compromise leucocyte function. In addition, ROS are important signalling molecules in the regulation of cellular homeostasis. It is important that anti-Nox2 therapy at the given dose will not supress essential cellular ROS production.

LMH001 (2,3,-dihydroxyphenyl) methyl 4-hydroxy-3-(hydroxyrnethyl) benzoate) is a small chemical compound (MW = 290.079)

belonging to a group of bi- and tri-aromatic compounds discovered previously [15]. It was found to have no cytotoxicity to cultured cells, but displayed a great inhibition of reactive oxygen species (ROS) production by endothelial cells in response to various pathogenic stimulations including AngII, TNFα and high glucose [15]. However, LMH001 was not tested in vivo previously. The overall aim of this study is to investigate the therapeutic potential of LMH001 against AngII-induced vascular oxidative stress and inflammatory damage to aortic walls using a disease model of AngII infusion-induced hypertension and aortic aneurysm in mice. Age matched p47phox knockout (p47KO) mice under exactly the same experimental conditions were used as control of Nox2 inhibition. Here, we reported that LMH001 is safe both in vitro and in vivo. When LMH001 was used at a small but effective dose that inhibited completely vascular oxidative stress in response to AngII challenge, the leucocyte oxidative response to pathogens was well preserved. LMH001 inhibited completely AngII-induced endothelial Nox2 activation, oxidative stress and inflammation, and protected mice from the development of hypertension and reduced incidence of aortic aneurysm formation in response to AngII infusion challenge. LMH001 has the potential to be developed into a new class of drug to treat oxidative stress.

1. Materials and methods

1.1. Reagents

LMH001 (2,3,-dihydroxyphenyl) methyl 4-hydroxy-3-(hydroxyrnethyl) benzoate, MW = 290.079) (molecular grade) was synthesized at Tocris Biosciences (Bristol, UK) [15]. AngII was purchased from Sigma-Aldrich. Polyclonal antibodies against Nox1, Nox2, Nox4, p22phox, p40phox, p47phox, p67phox, rac1 and CD31 were from Santa Cruz Biotechnology. Antibodies to mouse CD45 and CD68 were from Abcam (UK). Antibodies to phospho-ERK1/2 (ERK1^{Thr202}/^{Tyr204} and ERK2$^{Thr185/Tyr187}$), phospho-p38MAPK$^{Thr180/Tyr182}$, and phospho-JNK$^{Thr183/Tyr185,\ Thr221/Tyr223}$ were from Sigma-Aldrich (UK). DHE (dihydroethidium) was purchased from Invitrogen (UK). The scrambled control peptide and Nox2tat ([H]-RKKRRQRRRCSTRVRRQL-[NH2]) were provided by PeptideSynthetics (PPR Ltd. Fareham, UK). All other reagents and chemicals were from Sigma-Aldrich (UK) unless stated.

1.2. Fluorescence polarization assay

The plasmid containing p47phox tandem SH3 domain (residues 156–285) subcloned into pGex-6p-1 was kindly provided by Dr Rittinger (Imperial College London, UK). GST and GST-p47phox were expressed in competent BL21 cells and affinity purified. FITC-labelled p22phox C-terminal proline-rich domain peptide (FITC-Ahx-PPTNPPPRPPAE, residues 151–162 of p22phox) was synthesized by Peptide Protein Research Ltd. (Hampshire, UK). The equilibrium dissociation constant (KD) was determined using 5 nM of FITC-p22phox peptide and GST-p47phox SH3 domain protein at concentrations from 0.001 to 1 μM by fluorescence polarization assay according to a published protocol and was detected using a fluorescence microplate reader (PHERAstar^{Plus}, BMG labtech, UK) [16,17]. The polarization values in millipolarization units (mP) were measured at an excitation wavelength 485 nm and an emission wavelength at 530 nm. GST-p47phox at 50 nM and FITC-p22phox at 5 nM were used for testing LMH001 dose-dependent competitive inhibition. IC50 was determined using nonlinear regression in GraphPad Prism software (version 8.2). The Ki was calculated based on the values of IC50 and KD using equation published previously [17].

1.3. COS-phox cells, COS-p22phox cells and gene transfection

COS-phox cells (COS7 cells with stable expression of gp91phox, p22phox, p47phox, and p67phox) and COS-p22phox cells [18] were kindly provided by Dr M. C. Dinauer (The Indiana University Medical Centre,

USA). The COS-p22phox cells were transiently co-transfected with WT p47phox, mutated p47phox (S303-4/379A) using lipofectamine plus (Invitrogen) as described previously [18,19]. Cells were used after 48 h of gene transfection.

1.4. Coronary microvascular endothelial cell (CMEC) isolation and culture

This was performed according to a method reported previously [20]. CMEC were isolated from the hearts of WT and p47KO mice, and cultured in DMEM supplemented with 10% FBS, EC growth supplement (30 μg/ml), epidermal growth factor (10 ng/ml), vascular endothelial growth factor (0.5 ng/ml), ascorbic acid (1 μg/ml), hydrocortisone (1 μg/ml), L-glutamine (2 mmol/L), penicillin (50 U/ml) and streptomycin (50 μg/ml). At passage 2, CMECs were detached and seeded at 10^5 cells/ml in T25 flask for the experiments. Next day, the culture medium was replaced with medium containing either AngII (100 nM, 24–48h) or saline as control with or without LMH001. Cells were then harvested for further experiments.

1.5. Bone marrow hematopoietic cells and peripheral blood mononuclear cell (PBMC) isolation

The bone marrow cells were isolated from mouse femurs and the red blood cells were lysed according to the protocol published previously [21]. Mouse PBMC were isolated from fresh whole blood as described previously [22]. Briefly, whole blood was collected in EDTA tubes, and PBMC were isolated by density centrifugation using OptiPrep™ gradient solution (Sigma-Aldrich). The red blood cells were lysed by addition of 2 mL H_2O for 30 s. PBMC were then resuspended in HBSS, kept on ice and used immediately for the experiments.

1.6. Cell viability and cytotoxicity assays

Cell viability was examined using CellTiter 96® AQ$_{ueous}$ One Solution Cell Proliferation Assay (MTS) (Promega, UK) according to manufacturer's instruction. The absorbances at 490 nm were recorded using a plate reader (Molecular Devices, UK). The cytotoxicity was examined using MTT assay kit (Sigma, UK) according to manufacturer's instruction. Briefly, cells were stimulated with vehicle or LMH001 in phenol red-free culture medium for 24 h. The medium was then replaced by 100 μL MTT solution (0.5 mg/mL in phenol red free medium). Following 2 h of incubation, the MTT solution was removed and the crystals formed were dissolved with 100 μL of DMSO and the absorbance was read at wavelength of 569 nm using a plate reader (Molecular Devices).

1.7. ROS measurement using five complementary assays

(1) Lucigenin (5 μM)-chemiluminescence in the presence of NADPH (100 μM) was used for detecting ROS generation by vascular cell or tissue homogenates using a 96 well microplate luminometer (BMG Lumistar, Germany) [23]; NADPH was omitted for detecting $O_2^{\cdot-}$ production by living PBMC (5×10^4 cells/well in suspension). For the comparison of enzyme inhibitor efficacies, individual inhibitor, i.e., L-NAME (N-nitroarginine methyl ester, 100 μM, a nitric oxide synthase inhibitor), rotenone (100 μM, a mitochondrial complex-1 enzyme inhibitor), diphenyleneiodonium (DPI) (20 μM, a flavoprotein inhibitor), apocynin (20 μM, a Nox2 inhibitor) and Nox2tat (10 μM, a specific peptide Nox2 inhibitor) was added into the wells loaded with endothelial homogenates and incubated for 10 min at room temperature before the measurement of ROS production. (2) DHE fluorescence HPLC assay with or without superoxide dismutase–polyethylene glycol (PEG-SOD) was used to detect ROS production in tissue or cell homogenates [3]. Separation of DHE, superoxide specific product 2-hydroxyethidium (2-OH-E) and ethidium was performed using a JASCO HPLC system equipped with both UV (UV-2077, Jasco) and fluorescence (FP-2020,

Jasco) detectors. (3) Superoxide dismutase (SOD, 200U/mL)-inhibitable cytochrome *c* reduction assay was used for detecting $O_2^{\cdot-}$ production [23], and (4) Amplex Red assay (Invitrogen Inc.) was used for detecting H_2O_2 production in the presence or absence of catalase (300 U/ml) as described previously [23].

In situ ROS production by aorta sections was detected by DHE (2 μM) fluorescence in the presence or absence of tiron (10 mM, a non-enzymatic $O_2^{\cdot-}$ scavenger) to confirm the detection of $O_2^{\cdot-}$. DHE fluorescence was detected using an Olympus BX61 fluorescence microscope system, and quantified from at least 5 random fields/section with 3 sections/sample and 6 animals/group [23].

1.8. Preclinical pharmacokinetic (PK) assessment and modelling of LMH001

For the PK study, male CD1 mice (Charles River Ltd, UK) at 3-4-month-old (body weight 25–30 g) were used for the study. LMH001 was injected via a tail vein into mice at 10 mg/kg (bolus dosing volume 5 mL/kg). Six mice/per time points were sacrificed at 0, 1, 2.5, 5, 15, 30, 60 min and then at 3, 6, 12 and 24h after iv injection. Blood samples were collected for plasma preparation. LMH001 was extracted using 100 μL of HCl (60 mM) and 800 μL ethyl acetate according to a published method [24]. LMH001 was detected using an Accela HPLC coupled to a linear ion-trap tandem mass spectrometry (LTQ-Orbitrap XL, Thermo-Fisher Scientific, UK) in negative ionization mode. LMH001 appeared as a single symmetrical peak around 4.7 min with selected transition at m/z of $289.0 \to 167.0 \pm 5.0$. PK modelling was performed using the commercial software package, Phoenix WinNonlin 8.1. The concentrations of plasma LMH001 detected at 1–30 min after iv injection were modelled as described previously by non-compartmental analysis [25]. The calculated parameters included peak concentration (C_{max}); $AUC_{1-30\ min}$ and $AUC_{0-\infty}$ (time 0 to infinity); elimination rate constant (kel), $t_{1/2}$, and plasma clearance (CL).

1.9. Animals and AngII minipump infusion

The animal studies were performed in accordance with the protocols approved by Ethics Committees of the University of Surrey and the University of Reading and the UK Home Office under the Animals Act (Scientific Procedures) 1986, UK. The p47^{phox} knockout (KO) mice on a 129sv background were obtained from the European Mouse Mutant Archive, and backcrossed to C57BL/6J for 10 generations in our institution as described previously [19]. These mice lacked phagocyte superoxide production and manifested an increased susceptibility to infection. Littermates of WT, p47^{phox} KO mice were bred in our animal unit from heterozygotes and genotyped. Animals were housed under standard conditions with a 12:12 light dark cycle and food and water were available *ad libitum*.

For AngII experiments, littermates of WT and p47^{phox} KO male mice (7-month-old) were randomly grouped into control versus AngII, and vehicle versus LMH001 treatment groups (n = 12/per group). Osmotic mini-pumps (Alza Corp) was planted under anaesthesia for delivering Ang II for 14 days. The dose of 0.8 mg/kg/d was selected based on the literature [3] and our pilot experiments that showed significant vascular oxidative stress and high blood pressure with minimum unexpected incidence. Control group was infused with saline. Treatment groups received either LMH001 (2.5 mg/kg/d) or vehicle (0.3% DMSO in saline) with a total volume of 100 μl by intraperitoneal injection (ip) at 10 a.m. (once per day). LMH001 dose was estimated according to IC50 obtained from CMEC and pharmacokinetic modelling.

1.10. BP, aortic aneurysm and metabolic assessments

BP was measured by a computer controlled non-invasive tail-cuff BP system (Kent Scientific Corporation, USA) on conscious mice (after one week of training) at 10 a.m., and recorded by the CODA program [26].

The levels of fasting serum liver alanine aminotransferase were measured using standard method of the ADVIA 2400 analyser (Siemens, UK). Food and water consumptions were measured daily and body weights were measured weekly as described previously [26]. Aortic aneurysm was defined as an increase of 50% or more in the maximum diameter of suprarenal aorta compared to saline-infused control mice as described previously [27]. The suprarenal aortic diameter and wall thickness were measured using ImageJ (National Institutes of Health, Bethesda, MD).

1.11. Aorta functional assessments (organ bath)

This was done exactly as described previously [26]. Freshly isolated thoracic aorta rings were cut 3–4 mm in length and suspended in an organ bath (ML0146/C–V, AD Instrument Ltd) containing 10 ml (37 °C) of Krebs-Henseleit solution (in mM: NaCl 118, KCl 4.7, KH_2PO_4 1.2, $MgSO_4$ 1.2, $CaCl_2$ 2.5, $NaHCO_3$ 25, glucose 12, pH 7.4) gassed with 95% O_2/5% CO_2. The maximal contractile response to KCl (50 mM) was assessed firstly. After washout and re-equilibration, aorta contractile response to phenylephrine (0.001–10 μM added cumulatively) was tested. The following experiments were set-up firstly to achieve 70% of phenylephrine-dose-dependent tension which allowed us to assess AngII-induced further tension increase that is ROS dependent. Acetylcholine acts through its receptor on the endothelial cell membrane to increase the intracellular concentration of calcium, which through calmodulin to activate endothelial nitric oxide synthase (eNOS) and to produce nitric oxide (NO). Endothelium-dependent relaxation to acetylcholine (ACh, 0.001–10 μM added cumulatively) and endothelium-independent vessel relaxation to an NO donor, sodium nitroprusside (SNP, 0.0001–1 μM added cumulatively), were tested in rings pre-constricted with PE to 70% of their maximal phenylephrine-induced contractile response [26].

1.12. Measurement of NO production and serum TNFα

The level of NO production was assessed by measuring the concentration of serum nitrite, which is one of the primary stable and nonvolatile breakdown products of NO using the Griess assay kit from Promega (UK), and the serum TNFα levels was detected using an ELISA kit (ThermoFisher, UK) according to manufacturer's instruction.

1.13. Immunoblotting

This was performed exactly as described previously using aorta tissue homogenates [23]. The α-tubulin detected in the same sample was used as a loading control. For the quantification of phosphorylation of MAPKs, the total level of the same protein (phosphorylated and unphosphorylated) was pre-tested and justified to achieve equal loading. The images were captured digitally using a BioSpectrum AC imaging system (UVP, UK), and the optical densities of the protein bands were normalized to the loading controls of the same samples and quantified.

1.14. MMP activity zymography and histology

MMP activity was measured *in situ* on aorta sections using the Enz-Chek Gelatinase/Collagenase Assay Kit according to the manufacturer's instructions (Molecular Probes) [3,28]. Proteolytic activity was detected as green fluorescence, and visualized under fluorescence microscopy. In gel zymography was performed as described previously using SDS-page containing 0.8 mg/mL gelatine (Sigma) and aorta homogenates [29]. All stock solutions for electrophoresis were made using electrophoresis grade reagents, filter sterilized and kept at 4 °C. Homogenates were freshly prepared on ice and centrifuged at 4 °C. Gel Protein equal loading was pre-checked for α-tubulin expression. H&E staining was used for vessel morphology. Verhoeff-Van Gieson staining was used for

visualizing elastin fibres, and Masson's trichrome staining was used for visualizing collagen using the protocols published previously [30,31]. Images were captured using Evos XL Core imaging system and analysed using ImageJ 1.41 software and Image-pro Plus.

1.15. Immunofluorescence microscopy

The experiments were performed exactly as described previously [3, 23]. All buffers and reagents were freshly prepared and kept on ice before use. Experiments were performed on ice. Primary antibodies were used at 1:200 dilution. BSA (2%) was used in the place of primary
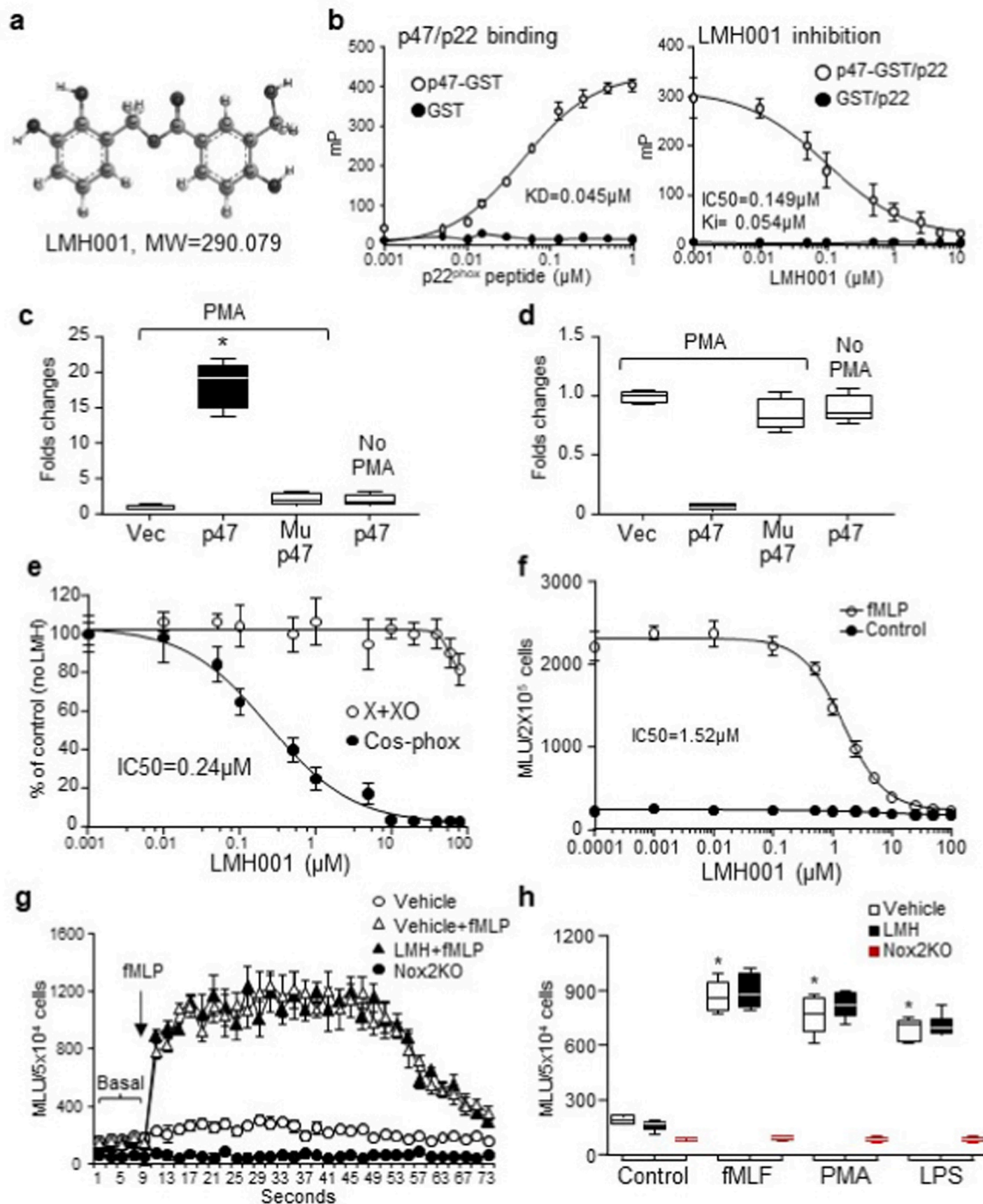
Fig. 1. LMH001 specificity and efficacy as p47^{phox} inhibitor. a. LMH001 structure. **b.** Kd and Ki values of LMH001 tested by fluorescence polarization. mP: millipolarization units. **c-d.** HPLC-MS/MS detection of LMH001 in COS-p22/p47^{phox} cells with or without PMA stimulation. **c.** LMH001 detected in p47^{phox} immunoprecipitation (IP) pellets. **d.** LMH001 detected in the fractions left after p47^{phox} IP. Mup47: p47^{phox} S303-4/379A mutation. Results were expressed as fold changes of Cos-p22^{phox} cells transfected with an empty vector (Vec) (values = 1). **e-h.** Lucigenin-chemiluminescence. **e.** $O_2^{.-}$ production by xanthine plus xanthine oxidase (X + XO) or PMA-stimulated COS-phox cells. **f.** $O_2^{.-}$ production by mouse peripheral blood mononuclear cells (PBMC). **g-h.** Oxidative burst response of PBMC isolated from mice after 14 d ip injection of LMH001. MLU: mean light units. *$P < 0.05$ for indicated values versus vehicle control values. n = 6 independent cell cultures or isolations.

antibodies as a negative control. Biotin-conjugated anti-rabbit or anti-goat IgG (1:1000 dilution) were used as secondary antibodies. Specific binding of antibodies was detected by extravidin-FITC or streptavidin-Cy3. Images were acquired either with Zeiss confocal fluorescence microscope or an Olympus BX61 fluorescence microscope system. Fluorescence intensities were quantified digitally using the software of the microscopy. For statistical analysis, at least 5 random fields/section with 3 sections/sample were used per animal and 6 animals were used per group. The control background captured from sections of the same aorta without primary antibody was deducted and the results were expressed as Fluo-intensity.

1.16. Statistical analysis

This was performed using GraphPad Prism software (version 8.2). Non-linear regression was used for the analysis of dose response of competitive inhibition and data were presented as Mean $\pm$ SD unless stated in the figure legends. One-way ANOVA plus the Brown-Forsythe test and Bartlett's test for examining the homogeneity of variance were used when there was only one factor or independent variable involved. Bonferroni's multiple comparison test was used for statistic differences in one-way mode. Two-way ANOVA plus Tukey's multiple comparison test were used for repeated measures such as body weight, heart weight, food and water intakes etc. and for studies where the effects of two independent variables were involved. The number of mice with or without aortic aneurysm in different groups was analysed using Fisher's exact test. For in vitro studies, results were from at least 5 independent cell cultures or cell isolations. Pharmacokinetic experiments were n = 6 mice/time point. AngII studies were n = 12 mice/group. For box-whisker graphics the medians plus minimum to maximum values were used. P < 0.05 was considered statistically significant.

2. Results

2.1. Background information of LMH001 action and efficacy

LMH001 is a small chemical with a molecular weight = 290.079 Da (Fig. 1a). It was designed based on published crystalised structure of p47[phox] tandem SH3 domains (PDBe 1ov3) by computer structural modelling of p47[phox] phosphorylation-induced conformational changes and interaction with p22[phox] C-terminal proline rich region peptide (QPPSNPPPRPP) as reported previously [32]. A pharmacophore was identified in p47[phox] within the space of Trp263, Asp243 and Ser208, which are the binding sites for p22[phox] (Supplementary Figs. 1a–b). LMH001 is designed as a bi-aromatic compound with modelled interacts with Ser208, Asp243, Glu241 and Asp261 via side-chain hydrogen bonding and with Trp-263 by π-π stacking (Supplementary Fig. 1c). When p47[phox] is phosphorylated and exposes the tandem SH3 binding pocket, LMH001 (due to its small size) can quickly occupy the pocket and block binding to p22[phox] and thereafter inhibit Nox2 activation (Supplementary Fig. 1d).

The efficacy of LMH001 as a competitive inhibitor to block phosphorylated p47[phox] binding to p22[phox] was examined by fluorescence polarization assay [16] using a GST fusion protein of p47[phox] tandem SH3 domains [33] and a FITC-labelled p22[phox] C-terminal proline-rich peptide (Fig. 1b). The equilibrium dissociation constant (KD) of p47[phox] binding to p22[phox] peptide was 0.045 μM. LMH001 inhibited competitively the binding between p47[phox] and p22[phox] peptide with an IC50 = 0.149 μM and a Ki = 0.054 μM.

The specificity of LMH001 binding to phosphorylated (but not unphosphorylated) p47[phox] was examined by co-immunoprecipitation (IP) using COS-p22/p47[phox] cells containing either a WT p47[phox] plasmid or a S303-304/309A mutated p47[phox] plasmid, in which the serines 303–304 and 379 were replaced by alanines that cannot be phosphorylated to expose the tandem SH3 pocket for LMH001 to bind [19,32]. Cells were challenged by PMA (100 ng, 1h) to induce p47[phox]

phosphorylation in the presence of LMH001 (10 μM). LMH001 was detected by HPLC-MS/MS only in the p47[phox] IP pellets of cells stimulated with PMA, but not in the IP pellets of mutated p47[phox] or unphosphorylated p47[phox] (no PMA stimulation) (Fig. 1c). LMH001 left in the tubes after IP was shown in Fig. 1d.

LMH001 was tested for non-specific anti-oxidant effect on $O_2^{\cdot-}$ production by xanthine plus xanthine oxidase. AngII-induced COS-phox cell $O_2^{\cdot-}$ production was examined in parallel for comparison (Fig. 1e). We found that when used above 50 μM, LMH001 started to display a weak anti-oxidant activity on $O_2^{\cdot-}$ production by xanthine plus xanthine oxidase. However, the IC50 of LMH001 to inhibit PMA-induced COS-phox cell $O_2^{\cdot-}$ production was 0.24 μM. There was a big gap (>200 times) between two concentrations.

2.2. In vitro and in vivo tests of LMH001 safety and pharmacological property

The effect of LMH001 on leucocyte $O_2^{\cdot-}$ burst response was examined using freshly isolated mouse PBMC (5×10^4 cells/test). Cells were challenged acutely with fMlP (10 μM) in the presence of LMH001 at the dose indicated, and were detected immediately for $O_2^{\cdot-}$ production by lucigenin-chemiluminescence. The IC50 of LMH001 to inhibit PBMC oxidative burst was 1.52 μM. (Fig. 1f). However, the effective dose that we used for treating AngII-induced hypertension in vivo was 2.5 mg/kg/day (ip) (see result subsections below) and the calculated highest blood concentration of LMH001 was <0.01 μM, which was too low to have an effect on PBMC oxidative burst.

The safety of LMH001 on leucocyte function was further tested in vivo. Mice were injected intraperitoneally (ip) LMH001 (5 mg/kg/d) for 14 days. Control mice were injected with vehicle. PBMC were isolated from these mice and tested immediately for their oxidative burst response to fMLP, or PMA or bacterial lipopolysaccharides (LPS) (Fig. 1g and h). There was no difference between vehicle and LMH001 treated mice for their PBMC oxidative response to fMLP, PMA or LPS. In contrast, PBMC isolated from Nox2KO mice had no oxidative burst response at all.

LMH001 used up to 100 μM showed no cytotoxicity to primary mouse bone marrow hematopoietic cells (BMHC) (Supplementary Fig. 2a). LMH001 (20 μM, 48h) had no cytotoxicity to human hepatic cells (HPG2), human neutrophils (HL-60), human pulmonary microvascular endothelial cells (HPMEC), human PBMC and rat embryonic cardiomyocytes (H9C2) (Supplementary Figs. 2b–c). Mouse primary coronary microvascular endothelial cells (CMEC) cultured with LMH001 for 14 days showed healthy tubulin stain and morphology (Supplementary Fig. 2d).

Intraperitoneal (ip) injection of LMH001 (5 mg/kg/d, once) for 14 days showed no toxicity to mice as demonstrated by food and water intakes, body weight, blood pressure (BP), heart rates, fasting blood glucose, levels of serum liver alanine aminotransferase, the proliferation of BMHC and the proportion of CD34 positive cells in BMHC (Supplementary Fig. 3).

Preclinical pharmacokinetic test of LMH001 was done in mice by bolus iv injection (10 mg/kg). LMH001 concentrations in the tissues were detected by HPLC-MS/MS and the results were analysed and modelled using software Phoenix WinNonlin 8.1. LMH001 displayed a short half-life ($t_{1/2} = 0.042$ h), rapid serum clearance and good tissue distribution (CL = 5682.63 mL/h/kg and VD = 343.43 ml/kg) (Table 1).

2.3. AngII-induced endothelial cell ROS production

AngII is a potent activator of endothelial NADPH oxidase [3,9]. The efficacy of LMH001 inhibiting AngII-induced endothelial Nox2 activation and $O_2^{\cdot-}$ production was examined firstly using primary mouse CMEC with an IC50 = 73.5 ng/mL (0.25 μM) (Fig. 2a). LMH001 (10 μM) demonstrated stronger inhibition on AngII-induced $O_2^{\cdot-}$ production by CMEC than apocynin (20 μM) or a peptide Nox2 inhibitor, Nox2-ds-tat

Table 1
Pharmacokinetic characterization of LMH001.

Parameter	Unit	NCA (0–30 min)
C_0	ng/mL	54593.44
C_{max}	ng/mL	27271.79
$AUC_{0-\infty}$	ng/mL/h	1759.75
$t_{1/2}$	h	0.042
Kel	1/h	16.55
CL	mL/h/kg	5682.63
Vd	mL/kg	343.43

NCA: non-compartmental analysis ($R^2 = 0.9575$). C_0: extrapolated plasma concentration at time 0; C_{max}: maximum plasma concentration; $AUC_{0-\infty}$: Area under the curve from time 0 extrapolated to infinite time; $t_{1/2}$: terminal half-life; Kel: elimination rate constant; CL: plasma clearance; Vd: volume of distribution.

(Nox2tat, 10 μM) [34] (Fig. 2b).

As an independent approach, LMH001 inhibition of AngII-induced endothelial $O_2^{\cdot-}$ production were further examined by DHE fluorescence HPLC assay using human pulmonary microvascular endothelial cells (HPMEC). LMH001 (5 μM) inhibited completely the production of $O_2^{\cdot-}$ (2-HE$^+$) (Fig. 2c, left panel) without significant effect on the production of other forms of ROS (E$^+$) (Fig. 2c, right panel), which further confirmed the specificity of LMH001 inhibition on Nox2-derived $O_2^{\cdot-}$ production.

The p47^{phox} is essential for Nox2 enzyme to produce $O_2^{\cdot-}$ in cells in response to challenges [1,35]. In order to confirm the effect of LMH001 on reducing AngII-induced endothelial oxidative stress was p47^{phox}-dependent, CMEC were isolated from WT and p47KO mice, stimulated with AngII in the presence or absence of LMH001 (5 μM) for 24 h and examined for $O_2^{\cdot-}$ productions (Fig. 2d). We found that LMH001 inhibited completely AngII-induced $O_2^{\cdot-}$ production by WT CMEC without significant effect on $O_2^{\cdot-}$ production by p47KO cells. $O_2^{\cdot-}$ is short lived and can be quickly converted to H_2O_2. We also examined the levels of H_2O_2 production by WT and p47KO CMEC and found that LMH001 inhibited completely AngII-induced H_2O_2 production by WT CMEC without significant effect on the levels of H_2O_2 production by p47KO cells (Fig. 2e).

Nox2 is barely expressed in aortic vascular smooth muscle cells
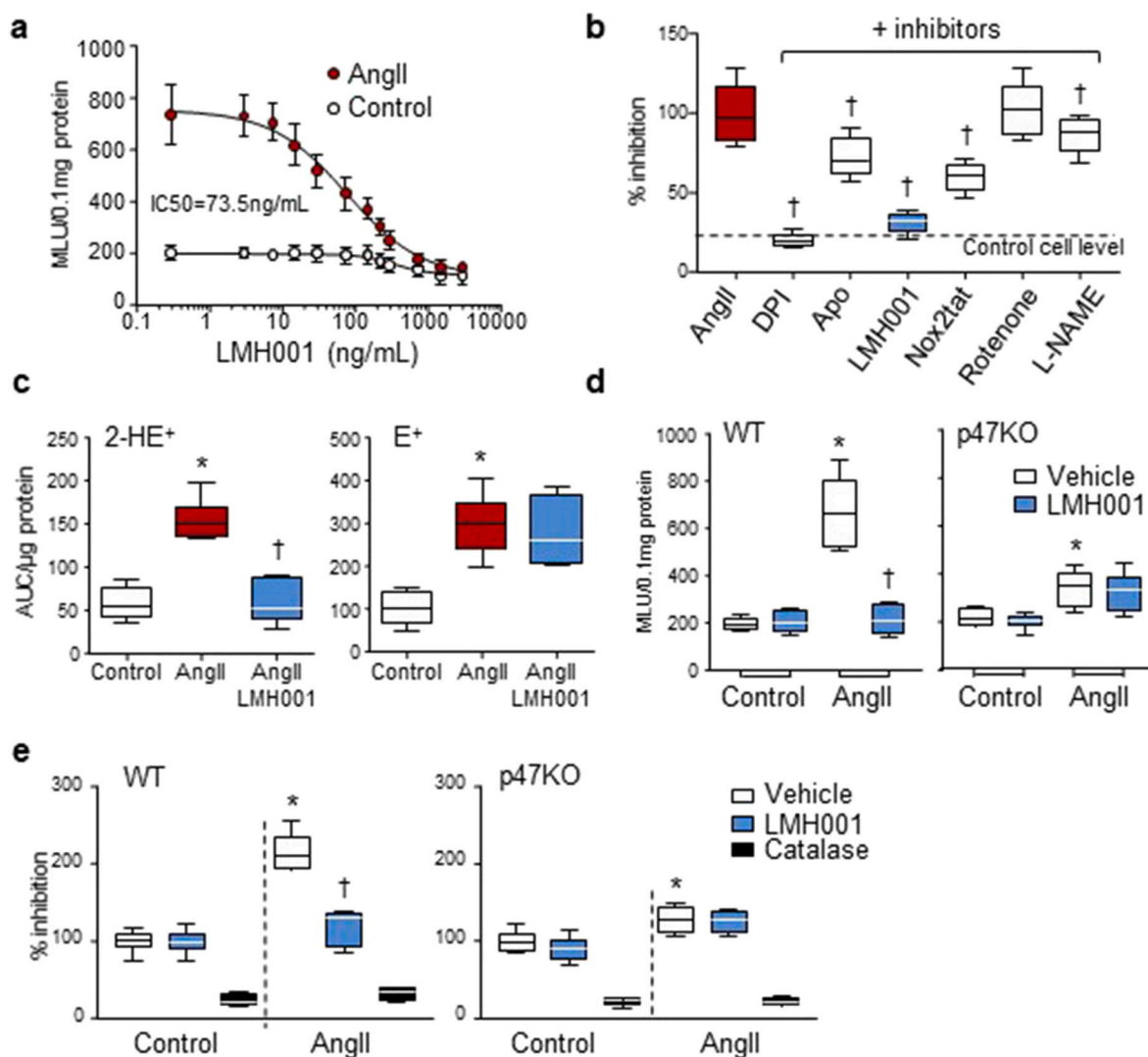
Fig. 2. LMH001 inhibition of AngII-induced endothelial cell ROS production. a,b,d: lucigenin-chemiluminescence. **a.** Dose response of LMH001 inhibition of AngII-induced $O_2^{\cdot-}$ production by primary mouse coronary microvascular endothelial cells (CMEC). MLU: mean light units. **b.** Effects of different inhibitors on AngII-induced $O_2^{\cdot-}$ production by WT CMEC. Results were expressed as % of AngII values (100%). **c.** DHE fluorescence HPLC detection of ROS production by human pulmonary microvascular endothelial cells. 2-HE+ ($O_2^{\cdot-}$), E+ (other ROS). AUC: area under curve, **d.** $O_2^{\cdot-}$ production by WT and p47^{phox} KO CMEC. **e.** H_2O_2 production by WT and p47^{phox} KO CMEC detected by amplex red assay. Results were expressed as % of vehicle control values (100%). *P < 0.05 for indicated values versus vehicle control (or control) values. †P < 0.05 for indicated values versus vehicle AngII (or AngII) values. n = 6 independent cell cultures. (For interpretation of the references to colour in this figure legend, the reader is referred to the Web version of this article.)

(VSMC) [36]. In response to AngII stimulation, VSMC generated excessive ROS, which were mainly from other Noxes or other enzymatic resources [36]. In order to confirm that LMH0001 is not a AT1 receptor antagonist, we tested LMH001 effect on AngII-induced ROS production by aortic VSMC (Supplementary Fig. 4). We found that 24 h of AngII stimulation induced 2.2 ± 0.3-fold increases in H_2O_2 production by VSMC, which were not inhibited by LMH001 However, there was a mild increase in $O_2^{\cdot-}$ production by VSMC in response to AngII stimulation, which was inhibited by LMH001 treatment.

2.4. AngII-induced hypertension & aortic aneurysm

The effect of LMH001 on AngII-induced oxidative stress, hypertension and aortic inflammation was examined in vivo using male mice (7-month-old). The littermates of age-matched p47KO mice under the same experimental conditions were used as controls for Nox2 inhibition. Mice were infused with AngII (0.8 mg/kg/d, mini-pump) for 14 days and treated with either LMH001 (ip, 2.5 mg/kg/d) or vehicle. The BP was measured every other day. The BP of WT AngII group increased rapidly and reached a stable plateau of 185 ± 7 mmHg at day 7 (Fig. 3a, left panel). However, in the p47KO mice, AngII-infusion only caused a mild but still significant increase in BP, and this was not affected by LMH001 treatment (Fig. 3a, middle panel and 3b). LMH001 effect on BP was rapid and reversable. When LMH001 was stopped in the middle of AngII infusion, BP started to increase within 24h. When LMH001 was given after 7 days of AngII infusion, the BP went down within 24h (Fig. 3a, right panel). The statistical significances of LMH001 effects on AngII-induced high BP at day 14 were given in Fig. 3b. Overall, LMH001 treatment prevented completely AngII infusion-induced high BP in the WT mice.

LMH001 treatment reduced significantly the number of WT mice that developed aortic aneurysms after AngII infusion as indicated by the morphological changes of the abdominal aortas and the differences in maximum diameters of suprarenal aortas (Fig. 3c). There were 8/12 mice with visible aorta aneurysm in WT AngII group, but only 1/12 in AngII/LMH001 treatment group (p = 0.009) (Fig. 3c, Supplementary Table 2).

AngII infusion-induced aorta oxidative stress was demonstrated by increased levels of $O_2^{\cdot-}$ production detected by superoxide dismutase-inhibitable cytochrome *c* reduction assay, and this was inhibited down to the saline control levels by LMH001 treatment (Fig. 3d). Increased $O_2^{\cdot-}$ production reduced NO bioavailability and resulted in vessel constriction. We found that LMH001 had no effect on aortic contractile response to phenylephrine, but reduced significantly AngII-induced further tension increases suggesting that it was ROS dependent (Fig. 3e). Acetylcholine through its receptor and Ca^{++}/calmodulin pathway increases endothelial NO production by eNOS [37]. We found that AngII-infusion attenuated significantly endothelium-dependent aorta relaxation to acetylcholine indicating endothelial dysfunction, and this was prevented by LMH001 treatment or by knockout of p47^{phox} (Fig. 3f). Similar results were obtained for aortic ring relaxation to a NO donor, sodium nitroprusside (SNP) (Fig. 3g).

2.5. AngII-induced multi-organ oxidative stress & aorta damage

AngII-infused WT mice suffered from multiple organ oxidative stress as shown by increased $O_2^{\cdot-}$ production in the tissue homogenates of lung, liver, heart, brain, kidney, spleen, adipose tissue, aorta and bone marrow hematopoietic cells (Fig. 4a). However, AngII-induced excessive ROS productions in these major organs were prevented or significantly inhibited by LMH001 treatment or by knockout of p47^{phox}. We also examined the levels of serum nitrite, one of the primary stable and non-volatile breakdown products of NO (Fig. 4b). We found that the levels of serum nitrite were reduced remarkably in WT AngII mice, but were well reserved in LMH001 treated WT AngII mice. AngII-induced systemic inflammation was further demonstrated by significant increases (~4-

folds) in the levels of serum TNFα in WT AngII mice (Fig. 4c). However, these AngII-induced inflammatory responses were prevented by LMH001 treatment of WT mice or by knockout of p47^{phox}.

LMH001 inhibition of AngII-induced aortic wall oxidative stress in WT (but not p47KO) mice was further demonstrated *in situ* by dihydroethidium (DHE) fluorescence using aortic sections (Fig 5a). Accompanied with the aortic wall oxidative stress, AngII infusion increased remarkably the thickness of aortic walls and this was worsening in the presence of aneurysm as demonstrated histologically using transverse sections of suprarenal aortas (Fig. 5b). However, these pathological changes were prevented or significantly reduced by LMH001 treatment or by knockout of p47^{phox}. Oxidative stress had been reported to play a key role in matrix metalloproteinase (MMP) activation and aortic aneurysm formation in both patients [28] and experimental animal models [3,38]. We found that AngII infusion upregulated MMP activity as detected by both *in situ* zymography (Fig. 5c, left panels) and in gel zymography (Fig. 5c, right panels). However, these AngII-induced aortic wall oxidative damages were prevented or significantly inhibited by LMH001 treatment or by knockout of p47^{phox}.

AngII-induced oxidative damage to the architecture of the connective fibres within the aorta wall were demonstrated by the reduction and breakdown of elastin fibres shown by Verhoeff-Van Gieson staining (black) (Fig. 6a); a substantial increase in adventitial collagen components demonstrated by Massson's trichrome staining (blue) (Fig. 6b); and infiltration of CD68 positive leucocytes (red) detected by immunofluorescence (Fig. 6c). However, these AngII-induced pathological changes in the aortic walls were prevented or significantly inhibited by treatment with LMH001 or by knockout of p47^{phox}.
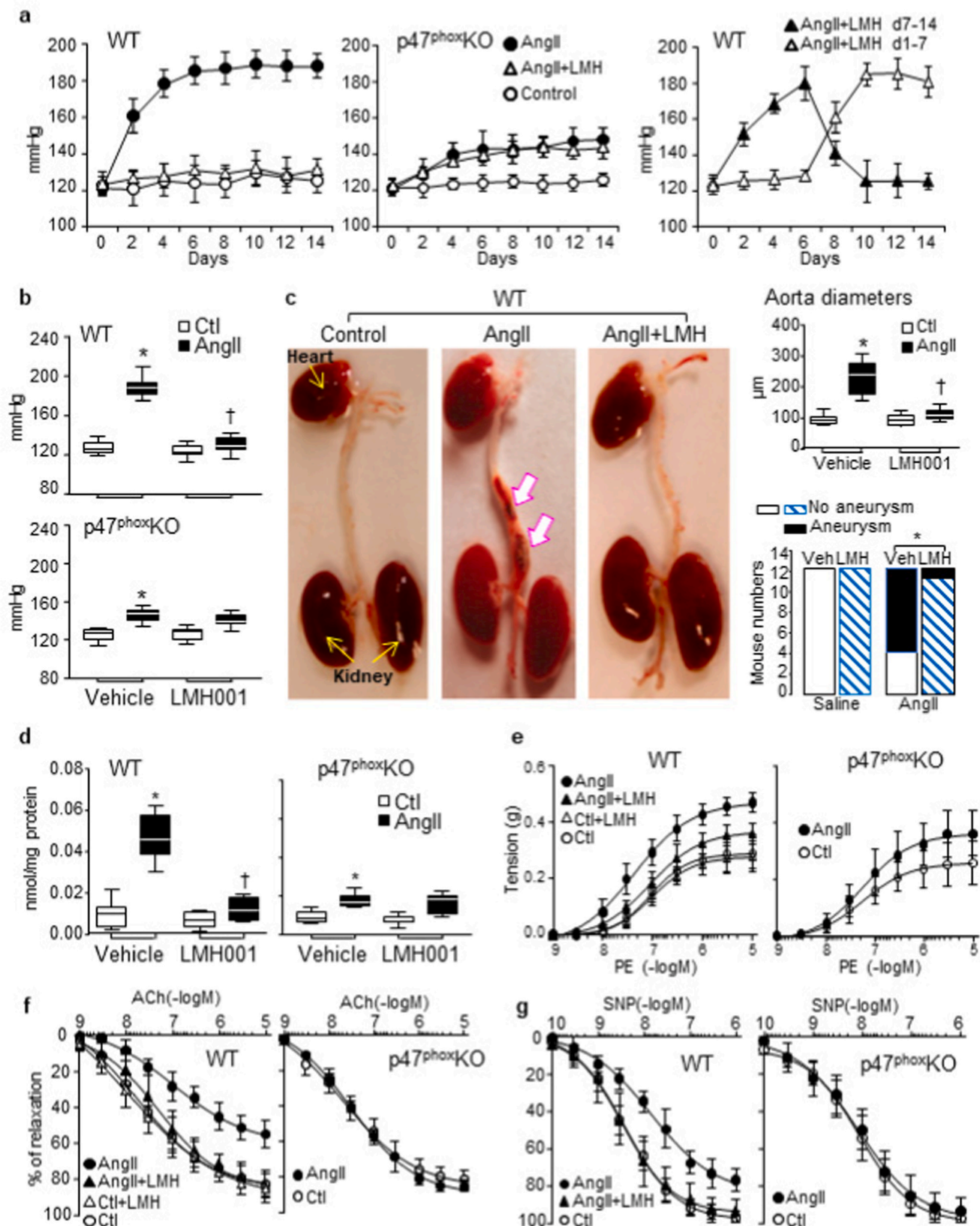
2.6. LMH001 inhibition of AngII-induced Nox2 & MAPK activation in aortic walls

The effects of LMH001 treatment on AngII infusion-induced aortic wall expression of Nox2, the activation of stress signalling molecule, i.e., ERK1/2 and inflammation were examined firstly *in situ* by immunofluorescence (Fig. 7). AngII infusion increased significantly the aortic wall expression of Nox2 (red) mainly in the endothelium and adventitia, and this was accompanied with an increase in ERK1/2 phosphorylation (green) (Fig. 7a). Accompanied with increased Nox2 (green) expression, there was significant infiltration of CD45 positive cells (red) within the aortic walls (Fig 7b). However, these AngII-induced changes were absent or significantly inhibited by LMH001 treatment or by knockout of p47^{phox}.

The effects of LMH001 on AngII-induced expression of Nox subunits and the activation of stress signalling pathways, i.e., MAPKs in the aortic wall were further examined by Western blots (Fig. 8). In comparison to control WT aortas, AngII-infusion increased significantly the levels of expressions of Nox2, p22^{phox}, p47^{phox}, p67^{phox} and rac1 in WT aortas (Fig. 8a), and these were accompanied by increased phosphorylation of ERK1/2, p38MAPK, and JNK (Fig. 8b). However, all these AngII-induced changes were significantly inhibited by LMH001 treatment. In p47^{phox} KO aortas, the basal (without AngII) expression of p40^{phox} was increased, which might be a compensatory response for the lack of p47^{phox}. AngII-infusion of p47KO mice increased markedly the expression of Nox1 and, to a much less extent, the Nox2 expression. However, there was no significant MAPK activation in response to AngII infusion in aortas of p47KO mice.

3. Discussion

Nox2-NADPH oxidase mediates many of the known pathophysiological effects of AngII in the cardiovascular system through the generation of excessive ROS [39–42]. However, common antioxidant therapies are not effective clinically, which might be due to the lack of specificity to inhibit ROS-generating enzymes [43,44]. Here, we reported for the first time that a novel small chemical compound

Fig. 3. LMH001 inhibition of AngII-induced hypertension, aortic aneurysm and aorta dysfunction in mice. a. LMH001 inhibition of AngII-induced blood pressure (BP) increases. Right panel: LMH001 (LMH) was given at day 7–14 (▲) or given at day 1–7 (△) of AngII infusion. **b.** BP after 14 days of AngII infusion. **c.** Aortic aneurysm (indicated by white arrows). Right upper panel: Maximum suprarenal aorta diameters. Right lower panel: Statistical analysis of aortic aneurysm incidences. *p = 0.009 by Fisher's exact test. **d.** Aorta $O_2^{\cdot-}$ production detected by superoxide dismutase-inhibitable cytochrome *c* reduction assay. **e-g.** Aortic ring organ bath. **e.** Constriction to phenylephrine (PE). **f.** Relaxation to acetylcholine (Ach). **g.** Relaxation to an NO donor, sodium nitroprusside (SNP). **b, c** (right upper panel) and **d** *P < 0.01 for indicated values versus vehicle (Veh) control (Ctl) values. †P < 0.01 for LMH001 values versus vehicle AngII values. n = 12 mice/group.
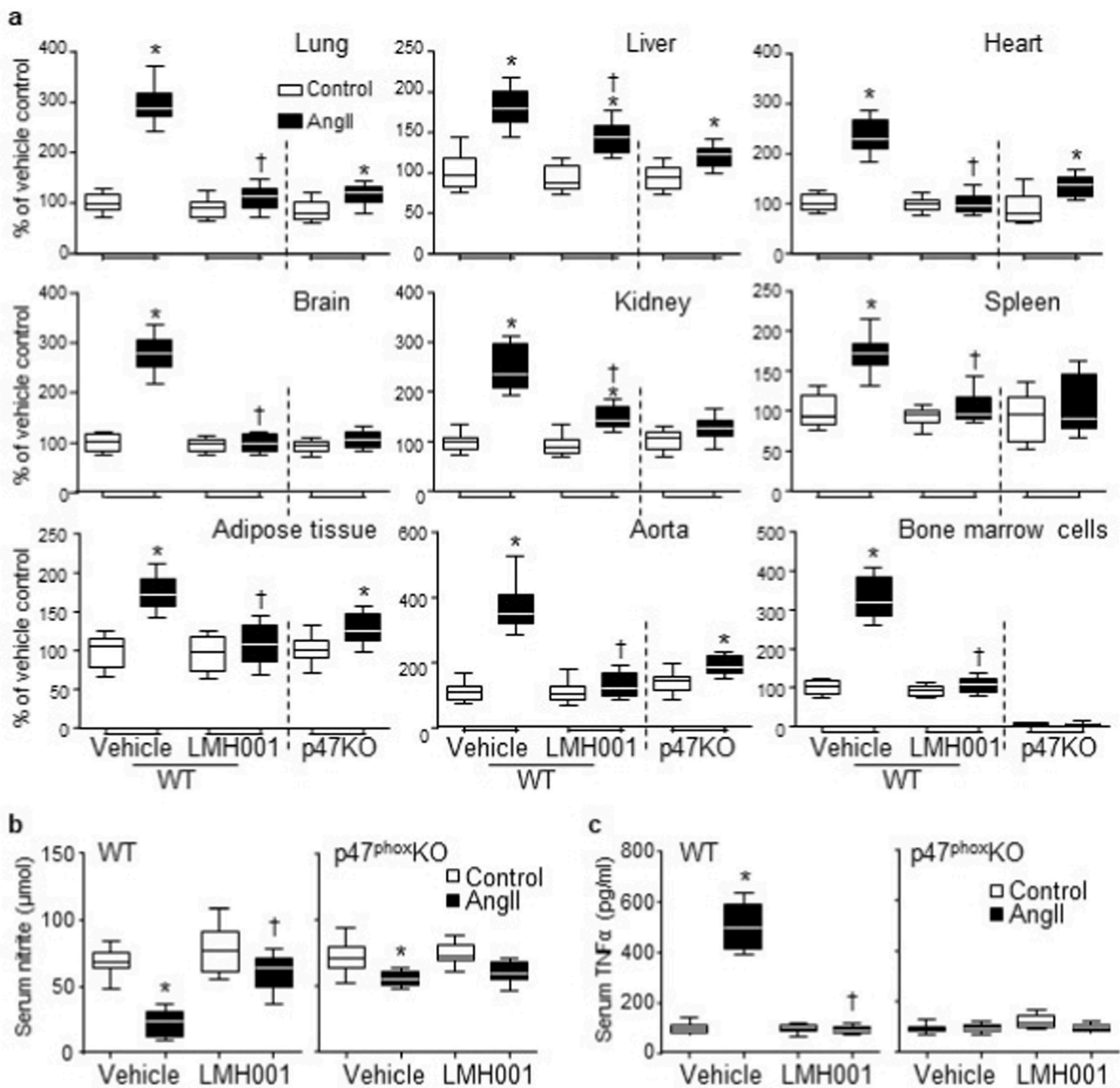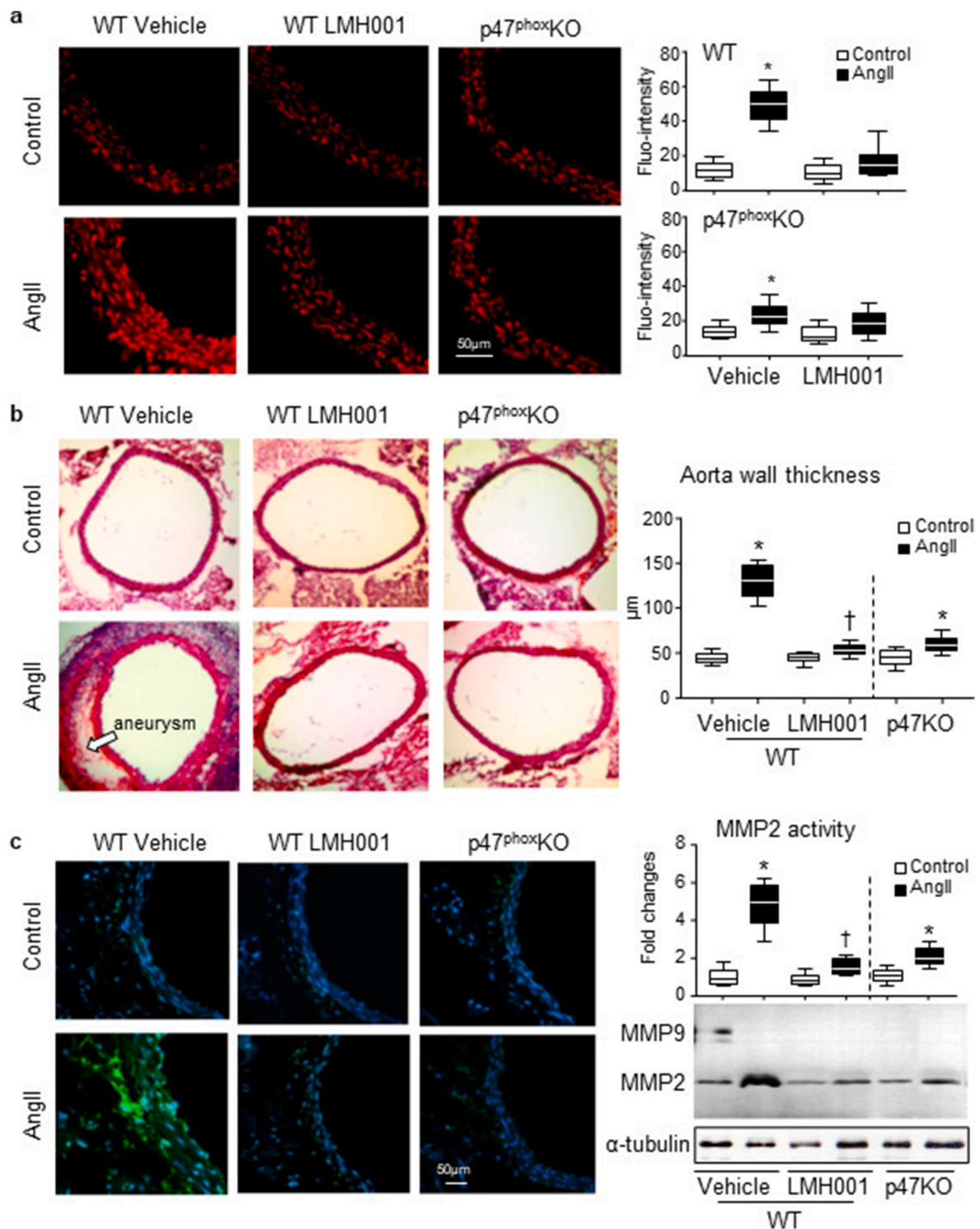
Fig. 4. LMH001 inhibition of AngII-induced multiple organ oxidative stress and inflammation. a. $O_2^{\cdot-}$ production detected by lucigenin-chemiluminescence in tissue homogenates of lungs, livers, hearts, brains, kidneys, spleens, adipose tissues, aortas and bone marrow cells. **b.** Levels of serum nitrite as a measure of NO production detected by Griess assay. **c.** Serum TNFα levels measured by ELISA. *P < 0.05 for indicated values versus vehicle control values in the same category labelled underneath. †P < 0.05 for indicated values versus AngII vehicle values. n = 12 mice/group.

(LMH001), by inhibiting phosphorylated p47phox interaction with p22phox, inhibited with high efficiency the excess ROS generation by endothelial cells that protected mice from multiple organ oxidative stress, inflammation and prevented the development of hypertension and aortic aneurysm in response to AngII infusion.

LMH001 is a very small chemical compound but showed stronger inhibition on AngII-induced endothelial ROS production in comparison to other current available chemical Nox2 inhibitors such as apocynin. When used at an effective dose for treating vascular oxidative stress, LMH001 displayed no significant effect on leucocyte function in response to pathogen challenges. In contrast, peripheral leukocytes or bone marrow hematopoietic cells isolated from p47KO or Nox2KO mice had no $O_2^{\cdot-}$ response at all. We believe the difference in LMH001 effects

between endothelial Nox2 and neutrophil Nox2 depended on the nature of the disease and the concentration of LMH001 used in the system. AngII-induced endothelial oxidative stress and dysfunction is a chronic process. However, pathogen-induced neutrophil oxidative burst involves large scale (>100 times more than in the vascular system) of Nox2 enzyme activation in seconds [8]. There is a large gap (therapeutic window) for LMH001 to be used at a small dose to treat vascular oxidative stress. The calculated serum concentration of LMH001 used in this study for treating AngII-induced vascular oxidative stress and hypertension was <0.01 μM, that was far too low to affect leucocyte oxidative burst.

Hypertension poses high risk for myocardial infarction, heart failure, stroke and renal diseases [45]. LMH001 displayed an excellent

Fig. 5. LMH001 inhibition of AngII-induced aorta ROS production, aortic wall thickness and MMP activation. a. *In situ* DHE fluorescence (red) detection of aorta ROS production. **b.** H&E staining for aortic aneurysm and morphology. Aorta wall thickness was measured using ImageJ software. **c.** Left panels: Representative images of *in situ* zymography detection of matrix metalloproteinase (MMP) activities (green fluorescence). Nuclei were labelled by DAPI (blue) to visualized cells. Right panels: In gel zymography detection of MMP activity. The optical densities of MMP2 bands were quantified, normalized to the loading control (α-tubulin) and expressed as fold changes against vehicle WT control values. *P < 0.05 for indicated versus vehicle control values. †P < 0.05 for indicated values versus vehicle AngII values. n = 9 mice/group. (For interpretation of the references to colour in this figure legend, the reader is referred to the Web version of this article.)

anti-hypertensive effect, which is mainly due to its inhibition on Nox2-derived ROS production by endothelial cells. Our study was properly controlled using WT versus p47KO mice under the same experimental settings. AngII-infusion of p47KO mice resulted in a moderate but significant increase in BP, which was not prevented by

LMH001. LMH001 anti-hypertensive effect was not due to off-target blockage of AT1 receptor because AngII-induced aortic smooth muscle H$_2$O$_2$ production was not affect by LMH001. However, it is important to note that this is only the first report and follow-up studies are needed to fully address the mechanisms of LMH001 on reducing vascular oxidative
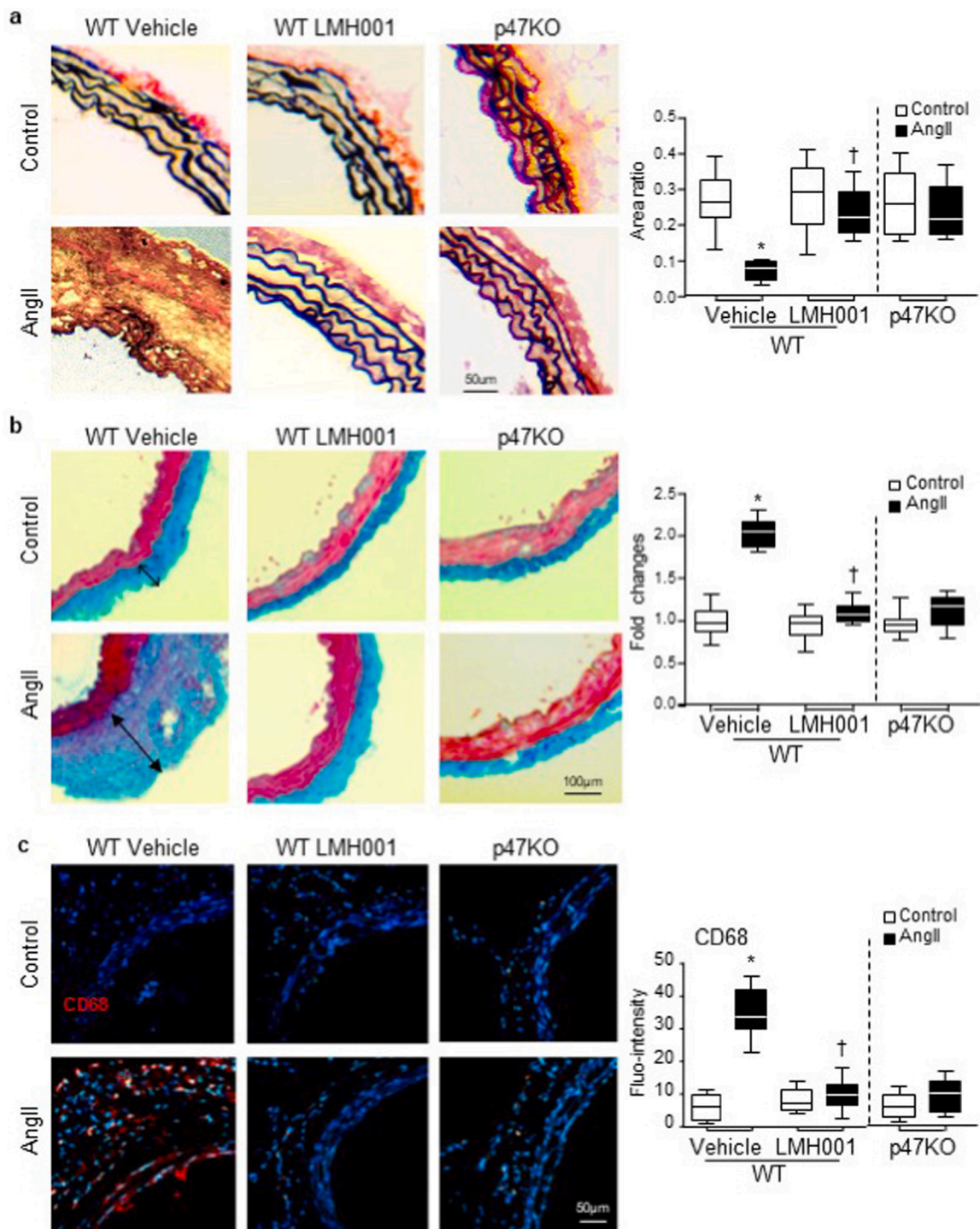
Fig. 6. LMH001 protection against AngII-induced damages to aortic elastin and collagen and inflammation. a. Verhoeff-Van Gieson staining of elastin (black). The results were expressed as ratios of elastin area/total vessel area. **b.** Masson's trichrome staining of collagen (blue). The results were expressed as fold changes of vehicle control values. **c.** Immunofluorescence detection of CD68 positive leucocyte (red) infiltration in aortic walls. Nuclei were labelled by DAPI (blue) to visualize the cells. *$P < 0.05$ for AngII values versus control values in the same category labelled underneath. †$P < 0.05$ for indicated LMH001 values versus AngII vehicle values. n = 9 mice/group. (For interpretation of the references to colour in this figure legend, the reader is referred to the Web version of this article.)

stress and hypertension.

Angiotensin-converting enzyme inhibitors (ACE-I) and AT1 receptor blockers are widely used as anti-hypertensive drugs to improve outcomes in patients with heart failure, diabetes mellitus, and myocardial infarction [46]. However, ACE-I can have significant non AngII side-effects of ACE inhibition such as cough, angioedema and hyperkalaemia [46–48]. AT1 receptor blockers share the same limitations as

ACE-I namely hyperkalaemia and high discontinuation in patients with chronic kidney disease who often have difficulty controlling hypertension despite multiple drug therapy [46–48]. LMH001, by inhibiting oxidative stress, represents a safe and effective complementary candidate for treating hypertension in addition to the current drug therapy to improve patient clinical outcomes.

Aortic dissection and aneurysm are serious medical conditions with
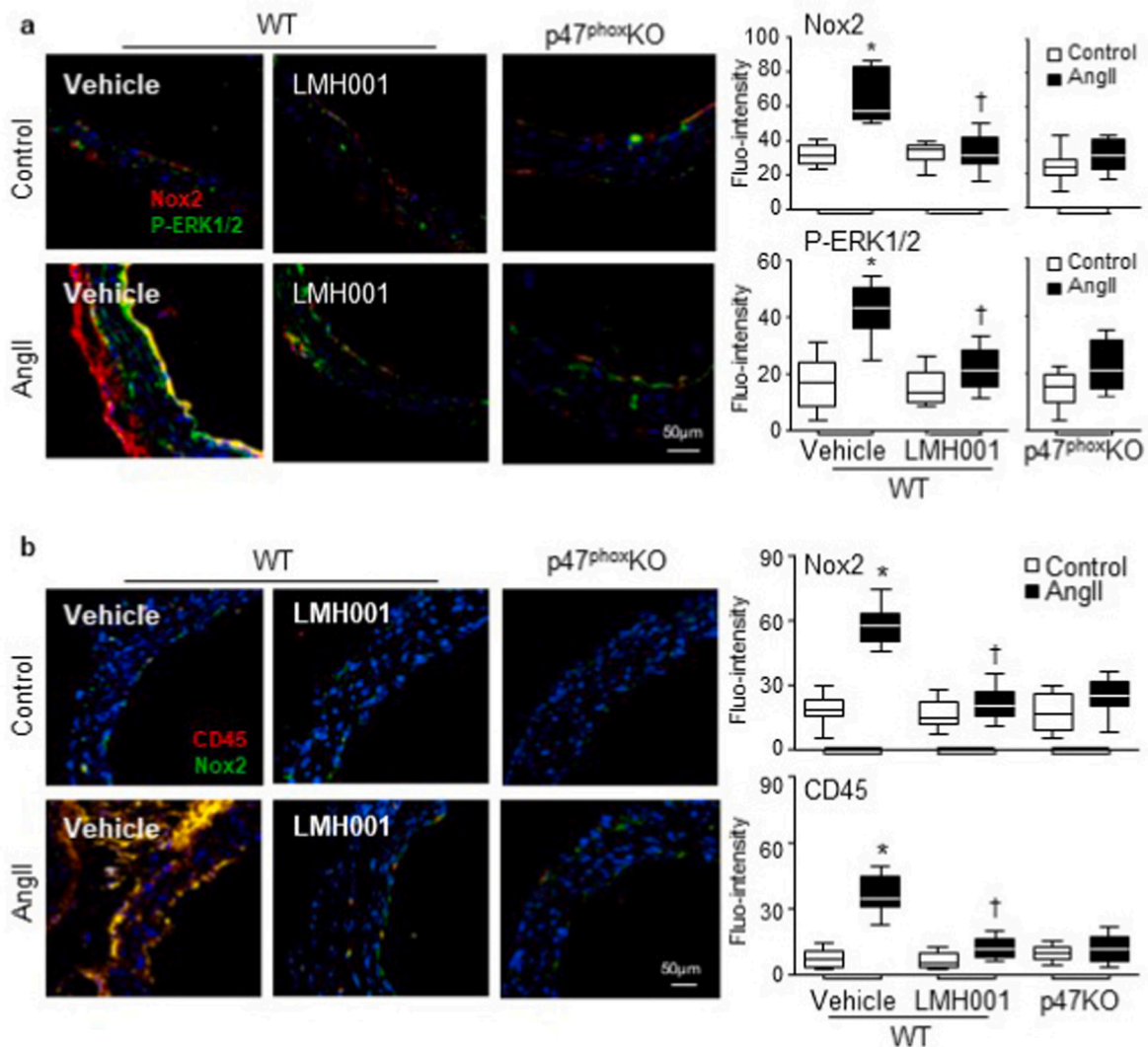
Fig. 7. LMH001 inhibition of AngII-induced Nox2 expression, ERK1/2 activation and CD45 positive cell infiltration in aortic walls detected by immunofluorescence. a. Nox2 expression (red) and ERK1/2 phosphorylation (green). **b.** Nox2 expression (green) and CD45 (red) positive leucocyte infiltration in aortic walls. Nuclei were labelled by DAPI (blue) to visualize the cells. Fluorescence intensities (Fluo-intensity) were quantified. *P < 0.05 for indicated values versus control values in the same category labelled underneath. †P < 0.05 for indicated LMH001 values versus AngII vehicle values. n = 9 mice/group. (For interpretation of the references to colour in this figure legend, the reader is referred to the Web version of this article.)

high mortality, and effective pharmacological treatment is still lacking. Recent studies have demonstrated an important role for endothelial Nox2 in aortic dissection and aneurysm formation that transgenic mice with endothelial specific overexpression of Nox2 increased the susceptibility to AngII-induced aorta dissection [3] and deletion of p47^{phox} could prevent AngII-induced aortic aneurysm [9]. Our mice used in this study were 7-month-old, which were more susceptible to AngII-induced vascular damage than mice at younger ages. Here we showed that LMH001 treatment inhibited AngII-induced endothelial oxidative stress and preserved endothelial function. Functional endothelium prevented leucocyte infiltration, protected aorta wall from AngII-induced oxidative damage, and reduced the incidence of aortic aneurysm.

In conclusion, we have reported in the current study that a novel small chemical compound, LMH001, by blocking phosphorylated p47^{phox} binding to p22^{phox}, inhibited AngII-induced Nox2-derived oxidative stress in endothelial cells with high efficiency and safety. Using an animal model of AngII-induced hypertension and aortic aneurysm, we showed that LMH001 used at a small dose (ip, 2.5 mg/kg/d) prevented AngII-induced multiple organ oxidative stress, inflammation; hypertension and reduced incidence of aortic aneurysm in mice.

LMH001 has the potential to be developed as a new class of drug therapy for oxidative stress-related cardiovascular diseases.

Author contributions

LMF: data acquisition and drafting the manuscript. FL: data acquisition and analysis. JD: data acquisition and analysis; LG: data acquisition and analysis; JML: study direction and critical review of the manuscript.

Data availability

Research material sources and all data that support the findings of this study are provided within this paper.
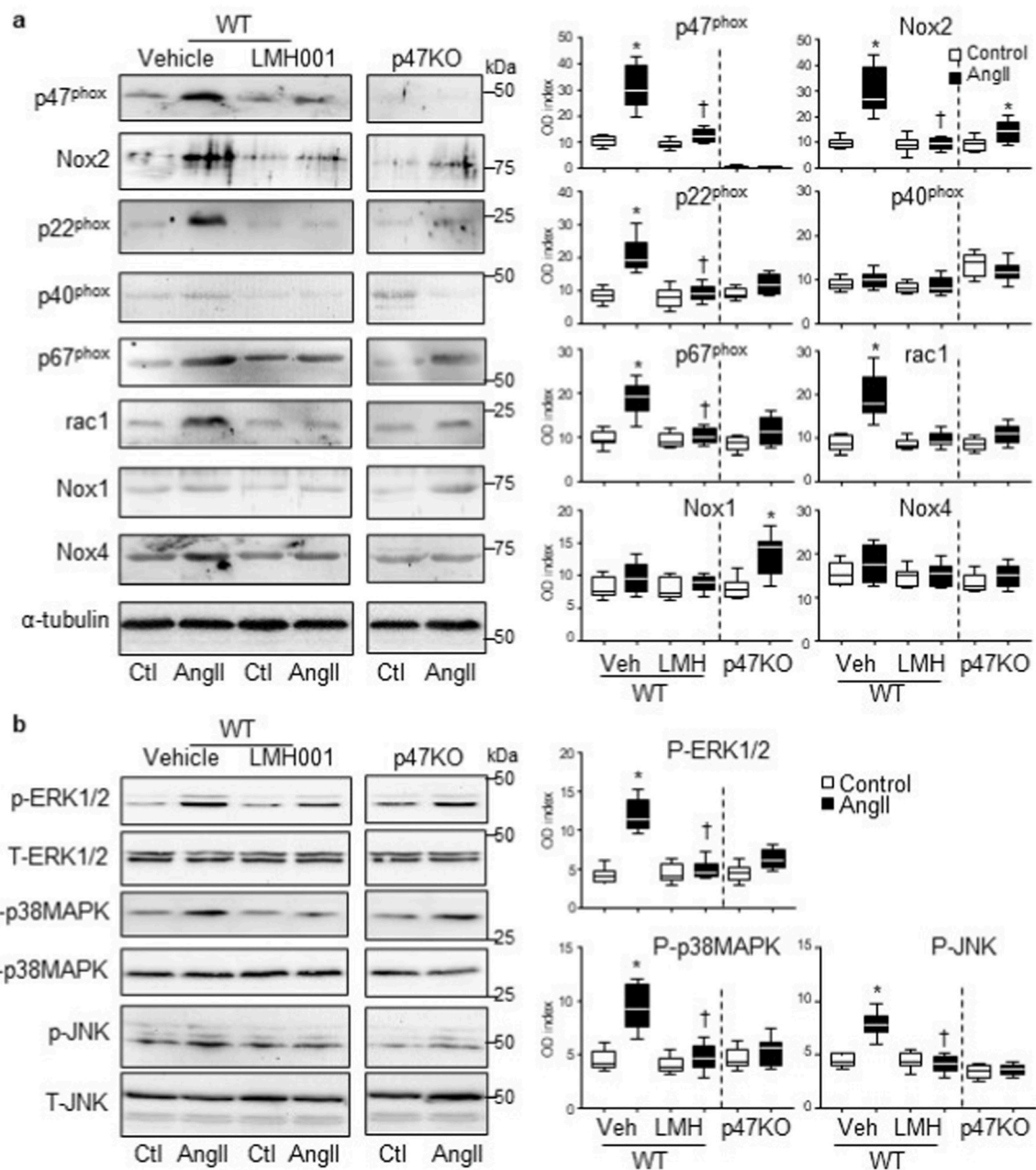
Fig. 8. Western blots for the expressions of Nox subunits and MAPK activation. a. Nox2 subunit expressions. **b.** Phosphorylation of ERK1/2, p38MAPKs and JNK. Optical densities (OD) of protein bands were quantified and normalized to α-tubulin detected in the same sample. For MAPK phosphorylation, the phospho-bands (P) were normalized to the total bands (T) of the same protein detected in the same samples and expressed as OD index (P/T). *P < 0.05 for indicated values versus vehicle (Veh) control (Ctl) values in the same category labelled underneath. †p < 0.05 for indicated values versus Veh AngII values. n = 9 mice/group.

Declaration of competing interest

None.

Appendix A. Supplementary data

Supplementary data to this article can be found online at https://doi.org/10.1016/j.redox.2022.102269.

References

[1] A. Vermot, I. Petit-Hartlein, S.M.E. Smith, F. Fieschi, NADPH oxidases (NOX): an overview from discovery, Molecular Mechanisms to Physiology and Pathology, Antioxidants (Basel) 10 (2021).

[2] F. Violi, R. Carnevale, L. Loffredo, P. Pignatelli, J.I. Gallin, NADPH oxidase-2 and atherothrombosis: insight from chronic granulomatous disease, Arterioscler. Thromb. Vasc. Biol. 37 (2017) 218–225.

[3] L.M. Fan, G. Douglas, J.K. Bendall, E. McNeill, M.J. Crabtree, A.B. Hale, A. Mai, J. M. Li, M.A. McAteer, J.E. Schneider, R.P. Choudhury, K.M. Channon, Endothelial cell-specific reactive oxygen species production increases susceptibility to aortic dissection, Circulation 129 (2014) 2661–2672.

[4] J.P. Taylor, H.M. Tse, The role of NADPH oxidases in infectious and inflammatory diseases, Redox Biol. 48 (2021) 102159.

[5] J.M. Li, A.M. Shah, Endothelial cell superoxide generation: regulation and relevance for cardiovascular pathophysiology, Am. J. Physiol. Regul. Integr. Comp. Physiol. 287 (2004) R1014–R1030.

[6] J. El-Benna, P.M. Dang, M.A. Gougerot-Pocidalo, J.C. Marie, F. Braut-Boucher, p47phox, the phagocyte NADPH oxidase/NOX2 organizer: structure, phosphorylation and implication in diseases, Exp. Mol. Med. 41 (2009) 217–225.

[7] J.M. Li, A.M. Mullen, S. Yun, F. Wientjes, G.Y. Brouns, A.J. Thrasher, A.M. Shah, Essential role of the NADPH oxidase subunit p47(phox) in endothelial cell

superoxide production in response to phorbol ester and tumor necrosis factor-alpha, Circ. Res. 90 (2002) 143–150.

[8] G.R. Drummond, S. Selemidis, K.K. Griendling, C.G. Sobey, Combating oxidative stress in vascular disease: NADPH oxidases as therapeutic targets, Nat. Rev. Drug Discov. 10 (2011) 453–471.

[9] M. Thomas, D. Gavrila, M.L. McCormick, F.J. Miller Jr., A. Daugherty, L.A. Cassis, K.C. Dellsperger, N.L. Weintraub, Deletion of p47phox attenuates angiotensin II-induced abdominal aortic aneurysm formation in apolipoprotein E-deficient mice, Circulation 114 (2006) 404–413.

[10] S. Altenhofer, K.A. Radermacher, P.W. Kleikers, K. Wingler, H.H. Schmidt, Evolution of NADPH oxidase inhibitors: selectivity and mechanisms for target engagement, Antioxidants Redox Signal. 23 (2015) 406–427.

[11] K. Hirano, W.S. Chen, A.L. Chueng, A.A. Dunne, T. Seredenina, A. Filippova, S. Ramachandran, A. Bridges, L. Chaudry, G. Pettman, C. Allan, S. Duncan, K. C. Lee, J. Lim, M.T. Ma, A.B. Ong, N.Y. Ye, S. Nasir, S. Mulyanidewi, C.C. Aw, P. P. Oon, S. Liao, D. Li, D.G. Johns, N.D. Miller, C.H. Davies, E.R. Browne, Y. Matsuoka, D.W. Chen, V. Jaquet, A.R. Rutter, Discovery of GSK2795039, a novel small molecule NADPH oxidase 2 inhibitor, Antioxidants Redox Signal. 23 (2015) 358–374.

[12] D.K. Johnson, K.J. Schillinger, D.M. Kwait, C.V. Hughes, E.J. McNamara, F. Ishmael, R.W. O'Donnell, M.M. Chang, M.G. Hogg, J.S. Dordick, L. Santhanam, L.M. Ziegler, J.A. Holland, Inhibition of NADPH oxidase activation in endothelial cells by ortho-methoxy-substituted catechols, Endothelium 9 (2002) 191–203.

[13] S.M. Smith, J. Min, T. Ganesh, B. Diebold, T. Kawahara, Y. Zhu, J. McCoy, A. Sun, J.P. Snyder, H. Fu, Y. Du, I. Lewis, J.D. Lambeth, Ebselen and congeners inhibit NADPH oxidase 2-dependent superoxide generation by interrupting the binding of regulatory subunits, Chem. Biol. 19 (2012) 752–763.

[14] F.C. Liu, H.P. Yu, P.J. Chen, H.W. Yang, S.H. Chang, C.C. Tzeng, W.J. Cheng, Y. R. Chen, Y.L. Chen, T.L. Hwang, A novel NOX2 inhibitor attenuates human neutrophil oxidative stress and ameliorates inflammatory arthritis in mice, Redox Biol. 26 (2019) 101273.

[15] J.-M. Li, B. Howlin, D.N. Meijles, W.I.P.O.I.B. (WIPO), in: Bi-aromatic and Tri-aromatic compounds as NADPH oxidase 2 (Nox2) inhibitors, 2013. https://patentscope.wipo.int/search/en/detail.jsf?docId=WO2013038136. International application published under the patent cooperation treaty.

[16] A.M. Rossi, C.W. Taylor, Analysis of protein-ligand interactions by fluorescence polarization, Nat. Protoc. 6 (2011) 365–387.

[17] Z. Nikolovska-Coleska, R. Wang, X. Fang, H. Pan, Y. Tomita, P. Li, P.P. Roller, K. Krajewski, N.G. Saito, J.A. Stuckey, S. Wang, Development and optimization of a binding assay for the XIAP BIR3 domain using fluorescence polarization, Anal. Biochem. 332 (2004) 261–273.

[18] M.O. Price, L.C. McPhail, J.D. Lambeth, C.H. Han, U.G. Knaus, M.C. Dinauer, Creation of a genetic system for analysis of the phagocyte respiratory burst: high-level reconstitution of the NADPH oxidase in a nonhematopoietic system, Blood 99 (2002) 2653–2661.

[19] L. Teng, L.M. Fan, D. Meijles, J.M. Li, Divergent effects of p47(phox) phosphorylation at S303-4 or S379 on tumor necrosis factor-alpha signaling via TRAF4 and MAPK in endothelial cells, Arterioscler. Thromb. Vasc. Biol. 32 (2012) 1488–1496.

[20] J.M. Li, A.M. Mullen, A.M. Shah, Phenotypic properties and characteristics of superoxide production by mouse coronary microvascular endothelial cells, J. Mol. Cell. Cardiol. 33 (2001) 1119–1131.

[21] X. Liu, N. Quan, Immune cell isolation from mouse femur, Bone Marrow, Bio Protoc 5 (2015).

[22] I. Mendez-David, Z. El-Ali, R. Hen, B. Falissard, E. Corruble, A.M. Gardier, S. Kerdine-Romer, D.J. David, A method for biomarker measurements in peripheral blood mononuclear cells isolated from anxious and depressed mice: beta-arrestin 1 protein levels in depression and treatment, Front. Pharmacol. 4 (2013) 124.

[23] L.M. Fan, L. Geng, S. Cahill-Smith, F. Liu, G. Douglas, C.A. McKenzie, C. Smith, G. Brooks, K.M. Channon, J.M. Li, Nox2 contributes to age-related oxidative damage to neurons and the cerebral vasculature, J. Clin. Invest. 129 (2019) 3374–3386.

[24] T.T. Zhang, Y.L. Wang, B. Jin, T. Li, C. Ma, Plasma pharmacokinetics of isorhapontigenin, a novel derivative of stilbenes, in mice by LC-MS/MS method, J. Asian Nat. Prod. Res. 21 (2019) 895–904.

[25] F. Liu, L.M. Fan, N. Michael, J.M. Li, In vivo and in silico characterization of apocynin in reducing organ oxidative stress: a pharmacokinetic and pharmacodynamic study, Pharmacol Res Perspect 8 (2020), e00635.

[26] J. Du, L.M. Fan, A. Mai, J.M. Li, Crucial roles of Nox2-derived oxidative stress in deteriorating the function of insulin receptors and endothelium in dietary obesity of middle-aged mice, Br. J. Pharmacol. 170 (2013) 1064–1077.

[27] H.Z. Amin, N. Sasaki, T. Yamashita, T. Mizoguchi, T. Hayashi, T. Emoto, T. Matsumoto, N. Yoshida, T. Tabata, S. Horibe, S. Kawauchi, Y. Rikitake, K.

[28] I. Hirata, CTLA-4 protects against angiotensin II-induced abdominal aortic aneurysm formation in mice, Sci. Rep. 9 (2019) 8065.

[28] S. Goodall, M. Crowther, D.M. Hemingway, P.R. Bell, M.M. Thompson, Ubiquitous elevation of matrix metalloproteinase-2 expression in the vasculature of patients with abdominal aneurysms, Circulation 104 (2001) 304–309.

[29] Z. Ren, J. Chen, R.A. Khalil, Zymography as a Research tool in the study of matrix metalloproteinase inhibitors, Methods Mol. Biol. 1626 (2017) 79–102.

[30] J. Wu, S.R. Thabet, A. Kirabo, D.W. Trott, M.A. Saleh, L. Xiao, M.S. Madhur, W. Chen, D.G. Harrison, Inflammation and mechanical stretch promote aortic stiffening in hypertension through activation of p38 mitogen-activated protein kinase, Circ. Res. 114 (2014) 616–625.

[31] A. Tanaka, T. Hasegawa, K. Morimoto, W. Bao, J. Yu, Y. Okita, Y. Tabata, K. Okada, Controlled release of ascorbic acid from gelatin hydrogel attenuates abdominal aortic aneurysm formation in rat experimental abdominal aortic aneurysm model, J. Vasc. Surg. 60 (2014) 749–758.

[32] D.N. Meijles, L.M. Fan, B.J. Howlin, J.M. Li, Molecular insights of p47phox phosphorylation dynamics in the regulation of NADPH oxidase activation and superoxide production, J. Biol. Chem. 289 (2014) 22759–22770.

[33] Y. Groemping, K. Lapouge, S.J. Smerdon, K. Rittinger, Molecular basis of phosphorylation-induced activation of the NADPH oxidase, Cell 113 (2003) 343–355.

[34] G. Csanyi, E. Cifuentes-Pagano, I. Al Ghouleh, D.J. Ranayhossaini, L. Egana, L. R. Lopes, H.M. Jackson, E.E. Kelley, P.J. Pagano, Nox2 B-loop peptide, Nox2ds, specifically inhibits the NADPH oxidase Nox2, Free Radic. Biol. Med. 51 (2011) 1116–1125.

[35] J.M. Li, S. Wheatcroft, L.M. Fan, M.T. Kearney, A.M. Shah, Opposing roles of p47phox in basal versus angiotensin II-stimulated alterations in vascular O2-production, vascular tone, and mitogen-activated protein kinase activation, Circulation 109 (2004) 1307–1313.

[36] B. Lassegue, K.K. Griendling, NADPH oxidases: functions and pathologies in the vasculature, Arterioscler. Thromb. Vasc. Biol. 30 (2010) 653–661.

[37] E. Zuccolo, C. Di Buduo, F. Lodola, S. Orecchioni, G. Scarpellino, D.A. Kheder, V. Poletto, G. Guerra, F. Bertolini, A. Balduini, V. Rosti, F. Moccia, Stromal cell-derived factor-1alpha promotes endothelial colony-forming cell migration through the Ca(2+)-dependent activation of the extracellular signal-regulated kinase 1/2 and phosphoinositide 3-kinase/AKT pathways, Stem Cell. Dev. 27 (2018) 23–34.

[38] G.K. Schwaerzer, H. Kalyanaraman, D.E. Casteel, N.D. Dalton, Y. Gu, S. Lee, S. Zhuang, N. Wahwah, J.M. Schilling, H.H. Patel, Q. Zhang, A. Makino, D. M. Milewicz, K.L. Peterson, G.R. Boss, R.B. Pilz, Aortic pathology from protein kinase G activation is prevented by an antioxidant vitamin B12 analog, Nat. Commun. 10 (2019) 3533.

[39] S. Higuchi, H. Ohtsu, H. Suzuki, H. Shirai, G.D. Frank, S. Eguchi, Angiotensin II signal transduction through the AT1 receptor: novel insights into mechanisms and pathophysiology, Clin. Sci. (Lond.) 112 (2007) 417–428.

[40] T. Kawai, S.J. Forrester, S. O'Brien, A. Baggett, V. Rizzo, S. Eguchi, AT1 receptor signaling pathways in the cardiovascular system, Pharmacol. Res. 125 (2017) 4–13.

[41] T. Munzel, T. Gori, J.F. Keaney Jr., C. Maack, A. Daiber, Pathophysiological role of oxidative stress in systolic and diastolic heart failure and its therapeutic implications, Eur. Heart J. 36 (2015) 2555–2564.

[42] B. Lassegue, A. San Martin, K.K. Griendling, Biochemistry, physiology, and pathophysiology of NADPH oxidases in the cardiovascular system, Circ. Res. 110 (2012) 1364–1390.

[43] MRC/BHF Heart Protection Study of antioxidant vitamin supplementation in 20,536 high-risk individuals: a randomised placebo-controlled trial, Lancet 360 (2002) 23–33.

[44] I.M. Lee, N.R. Cook, J.E. Manson, J.E. Buring, C.H. Hennekens, Beta-carotene supplementation and incidence of cancer and cardiovascular disease: the Women's Health Study, J. Natl. Cancer Inst. 91 (1999) 2102–2106.

[45] J. Kitt, R. Fox, K.L. Tucker, R.J. McManus, New approaches in hypertension management: a review of current and developing technologies and their potential impact on hypertension care, Curr. Hypertens. Rep. 21 (2019) 44.

[46] S. Bezalel, K. Mahlab-Guri, I. Asher, B. Werner, Z.M. Sthoeger, Angiotensin-converting enzyme inhibitor-induced angioedema, Am. J. Med. 128 (2015) 120–125.

[47] G. Bandak, Y. Sang, A. Gasparini, A.R. Chang, S.H. Ballew, M. Evans, J. Arnlov, L. H. Lund, L.A. Inker, J. Coresh, J.J. Carrero, M.E. Grams, Hyperkalemia after initiating renin-angiotensin system blockade: the stockholm creatinine measurements (SCREAM) project, J. Am. Heart Assoc. 6 (2017).

[48] Y. Qiao, J.-I. Shin, Y. Sang, L.A. Inker, A. Secora, S. Luo, J. Coresh, G.C. Alexander, J.W. Jackson, A.R. Chang, M.E. Grams, Discontinuation of angiotensin converting enzyme inhibitors and angiotensin receptor blockers in chronic kidney disease, Mayo Clin. Proc. 94 (2019) 2220–2229.